

NUMERICAL SIMULATION OF THERMAL PROCESSES  
PROCEEDING IN A MULTI-LAYERED FILM SUBJECTED TO  
ULTRAFAST LASER HEATING

EWA MAJCHRZAK

*Silesian University of Technology, Gliwice, Poland*  
*e-mail: ewa.majchrzak@polsl.pl*

BOHDAN MOCHNACKI

*Czestochowa University of Technology, Czestochowa, Poland*  
*e-mail: moch@imi.pcz.pl*

JÓZEF S. SUCHY

*AGH, University of Science and Technology, Cracow, Poland*  
*e-mail: jsuchy@agh.edu.pl*

In the paper, the mathematical model, numerical algorithm and examples of computations concerning thermal processes proceeding in a multi-layered thin film subjected to an ultrafast laser pulse are discussed. The equations describing a course of the analysed process correspond to the dual-phase-lag model and contain both the relaxation time  $\tau_q$  and additionally the thermalization time  $\tau_T$ . At the stage of numerical simulation, the finite difference method has been used. The algorithm is based on an artificial decomposition of the domain considered, while common thermal interactions between successive layers are taken into account using conditions of heat flux and temperature continuity at points corresponding to internal boundaries (1D task has been considered).

*Key words:* microscale heat transfer, thin films, laser pulse, numerical modelling

## 1. Introduction

Classical Fourier's equation constitutes a quite good mathematical description of heat conduction processes proceeding in macro domains subjected to external thermal interactions whose duration is not very short, at the same time the temperature considered  $T(x, t)$  should be essentially bigger than 0 K (Al-Nimr, 1997; Chen *et al.*, 2004; Escobar *et al.*, 2006; Özişik and Tzou, 1994; Tamma and Zhou, 1998). It is well known that the Fourier law assumes instan-

taneous heat propagation and this assumption leads to evident errors when the time considered is comparable with the relaxation time  $\tau_q$  of heat carriers (average time between successive electron-phonon collisions in the conductors or semiconductors and phonon-phonon collisions in dielectrics). Additionally, the Fourier equation is acceptable when the characteristic dimension  $L$  of the domain considered is essentially larger than the mean free path  $\Lambda$  of the heat carriers (the average distance that energy carriers travel between successive collisions). So, generally speaking, considering the processes proceeding in domains for which  $L \ll \Lambda$  (e.g. thin films) subjected to ultrafast heating (e.g. short-pulse laser interaction) other models of heat transport phenomena must be taken into account. The limitations concerning the Fourier model applications are discussed, among others, in Escobar *et al.* (2006), Özişik and Tzou (1994), Tamma and Zhou (1998).

In the paper, the problem of heat transfer proceeding in a multi-layered thin film subjected to a short pulse laser heating is considered. It should be pointed out that the heat transport through thin films is of vital importance in microtechnology applications (Dai and Nassar, 2001a,b; Smith and Norris, 2003). The mathematical description of the process discussed is based on the dual-phase-lag model presented, among others, in Escobar *et al.* (2006), Özişik and Tzou (1994), Tamma and Zhou (1998), Tzou (1995). Taking into account characteristic features of thin film geometry one can assume that the components of heat flux in macro-directions (e.g.  $x_2, x_3$ ) result from the traditional Fourier law, while in the definition of heat flux in the direction  $x_1$  the relaxation time  $\tau_q$  and additionally the thermalization time  $\tau_T$  (the mean time required for electrons and lattice to reach equilibrium) are introduced (Dai and Nassar, 2001). So, in this direction the heat flux and temperature gradient will occur at different times.

The mathematical model presented in the next section concerns a 1D problem corresponding to the micro-direction  $x_1 = x$  (heat fluxes in the directions  $x_2, x_3$  are neglected). For most short laser pulse interactions with thin films, the laser spot size is much larger than the film thickness. Therefore, it is reasonable to treat the interactions as a one-dimensional heat transfer process (Chen and Beraun, 2001).

At the stage of numerical realisation, an algorithm based on the finite difference method is applied, at the same time a certain concept of domain decomposition is proposed. Temporary temperature fields in successive layers are calculated separately, while the continuity conditions allow one to find the temporary solution concerning the entire domain. In the final part of the paper, examples of computations are shown.

### 2. Heat transport at the microscale

Heat transport equations describing thermal behaviour of a thin film, as shown in Fig. 1, can be written in the form (Dai and Nassar, 2000; Dai and Nassar, 2001; Özişik and Tzou, 1994; Tamma and Zhou, 1998; Tzou, 1995)

$$c \frac{\partial T(x, t)}{\partial t} = -\nabla \cdot \mathbf{q}(x, t) + Q(x, t) \tag{2.1}$$

and

$$q_1(x, t + \tau_q) = -\lambda \frac{\partial T(x, t + \tau_T)}{\partial x_1} \tag{2.2}$$

$$q_2(x, t) = -\lambda \frac{\partial T(x, t)}{\partial x_2} \qquad q_3(x, t) = -\lambda \frac{\partial T(x, t)}{\partial x_3}$$

where  $x = \{x_1, x_2, x_3\}$ ,  $\mathbf{q} = [q_1, q_2, q_3]^T$  is the heat flux,  $\lambda$  is the thermal conductivity,  $c$  is the volumetric specific heat,  $Q$  is the capacity of internal heat sources,  $\tau_T, \tau_q$  are the positive constants which are the time lags of the temperature gradient and heat flux, respectively.

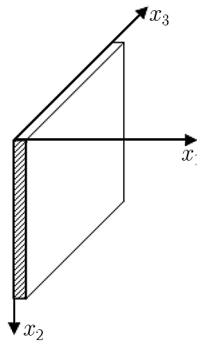


Fig. 1. Thin film

Using the Taylor series expansion, the following first-order approximation of equation (2.2)<sub>1</sub> can be taken into account

$$q_1(x, t) + \tau_q \frac{\partial q_1(x, t)}{\partial t} = -\lambda \left[ \frac{\partial T(x, t)}{\partial x_1} + \tau_T \frac{\partial}{\partial t} \left( \frac{\partial T(x, t)}{\partial x_1} \right) \right] \tag{2.3}$$

Equation (2.1), which in the case of 1D problem ( $x = x_1$ ) is of the form

$$c \frac{\partial T(x, t)}{\partial t} = -\frac{\partial q(x, t)}{\partial x} + Q(x, t) \tag{2.4}$$

where

$$q(x, t) + \tau_q \frac{\partial q(x, t)}{\partial t} = -\lambda \left[ \frac{\partial T(x, t)}{\partial x} + \tau_T \frac{\partial}{\partial t} \left( \frac{\partial T(x, t)}{\partial x} \right) \right] \quad (2.5)$$

should be supplemented by adequate boundary and initial conditions.

### 3. Multi-layered domain

Let us consider a multi-layered thin film of thickness  $L = L_1 + L_2 + \dots + L_M$  (as in Fig. 2) with the initial temperature distribution  $T(x, 0) = T_0$ , constant thermal properties of successive layers, ideal thermal contact between the layers and insulated external boundaries. The front surface  $x = 0$  is irradiated by a laser pulse whose output intensity equals  $I(t)$ . According to Tang and Araki (1999), the conduction heat transfer can be modeled by equation (2.4) with internal volumetric heat sources  $Q(x, t)$ , at the same time for  $x = 0$  the non-flux condition can be assumed. In this paper, the following formula (Kaba and Dai, 2005; Tzou and Chiu, 2001) has been applied

$$Q(x, t) = \sqrt{\frac{\beta}{\pi}} \frac{1 - R}{t_p \delta} I_0 \exp\left(-\frac{x}{\delta} - \sqrt{\beta} \frac{|t - 2t_p|}{t_p}\right) \quad (3.1)$$

where  $I_0$  is the laser intensity which is defined as the total energy carried by the laser pulse per unit cross-section of the laser beam,  $t_p$  is the characteristic time of the laser pulse,  $\delta$  is the characteristic transparent length of irradiated photons called the absorption depth,  $R$  is the reflectivity of the irradiated surface and  $\beta = 4 \ln 2$  (Chen and Beraun, 2001).

The local and temporary value of  $Q(x, t)$  results from the distance  $x$  between the surface subjected to laser action and the point considered. So, the following system of equations is taken into account

$$x \in \Omega_m : \quad c_m \frac{\partial T_m(x, t)}{\partial t} = -\frac{\partial q_m(x, t)}{\partial x} + Q_m(x, t) \quad m = 1, 2, \dots, M \quad (3.2)$$

$$q_m(x, t) + \tau_{qm} \frac{\partial q_m(x, t)}{\partial t} = -\lambda_m \left[ \frac{\partial T_m(x, t)}{\partial x} + \tau_{Tm} \frac{\partial}{\partial t} \left( \frac{\partial T_m(x, t)}{\partial x} \right) \right]$$

The boundary conditions on the contact surfaces between the sub-domains have the form of continuity ones, which means

$$x \in \Gamma_m : \quad \begin{cases} T_m(x, t) = T_{m+1}(x, t) \\ q_m(x, t) = q_{m+1}(x, t) \end{cases} \quad m = 1, 2, \dots, M - 1 \quad (3.3)$$

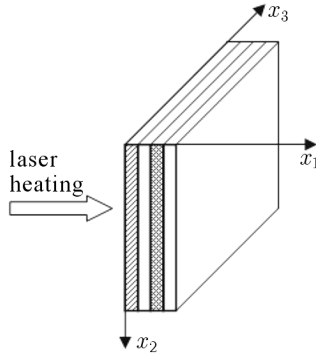


Fig. 2. Multi-layered domain

The initial conditions are assumed in the following way

$$t = 0 : \quad T_m(x, 0) = T_{m0} \quad \left. \frac{\partial T_m(x, t)}{\partial t} \right|_{t=0} = 0 \quad (3.4)$$

### 4. Numerical model

At the stage of numerical computations, the finite difference method has been used, while the final system of equations has been solved using the Thomas algorithm (Majchrzak and Mochnacki, 2004; Mochnacki and Suchy, 1995) (separately for successive layers).

To find a numerical solution to the problem discussed, a staggered grid is introduced (Dai and Nassar, 2000), as shown in Fig. 3. For convenience, we omit  $m$  and denote  $T_i^f = T(ih, f\Delta t)$ , where  $h$  is the mesh size,  $\Delta t$  is the time step,  $i = 0, 2, 4, \dots, N$ ,  $f = 0, 1, \dots, F$ , and  $q_j^f = q(jh, f\Delta t)$ , where  $j = 1, 3, \dots, N - 1$ .

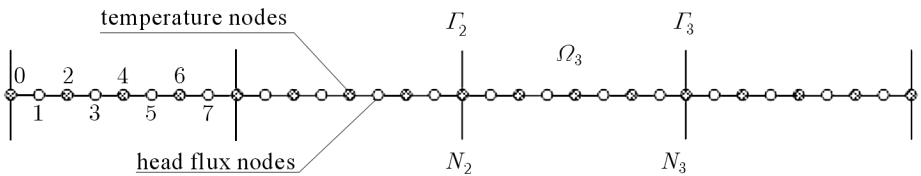


Fig. 3. Discretization

As was mentioned, the numerical procedure proposed is based on the Thomas algorithm for a tridiagonal linear system of equations and decomposition

of the domain into  $M$  sub-domains corresponding to successive layers. Additionally, an adequate procedure of contact temperatures computations is introduced.

Let us consider an internal point  $x_i \in \Omega_m$ . The finite difference approximation of equation (3.2)<sub>1</sub> can be written as follows (implicit scheme)

$$c_i \frac{T_i^f - T_i^{f-1}}{\Delta t} = -\frac{q_{i+1}^f - q_{i-1}^f}{2h} + Q_i \quad (4.1)$$

where the index  $i$  corresponds to 'temperature nodes' (Fig. 3) belonging to the  $\Omega_m$  sub-domain.

Equation (3.2)<sub>2</sub> can be transformed to the form

$$q_j^f + \tau_{qj} \frac{q_j^f - q_j^{f-1}}{\Delta t} = -\lambda_j \left( \frac{T_{j+1}^f - T_{j-1}^f}{2h} \right) - \frac{\lambda_j \tau_{Tj}}{\Delta t} \left( \frac{T_{j+1}^f - T_{j-1}^f}{2h} - \frac{T_{j+1}^{f-1} - T_{j-1}^{f-1}}{2h} \right) \quad (4.2)$$

or

$$q_j^f = \frac{\tau_{qj}}{\Delta t \left( 1 + \frac{\tau_{qj}}{\Delta t} \right)} q_j^{f-1} - \frac{\lambda_j \left( 1 + \frac{\tau_{Tj}}{\Delta t} \right)}{2h \left( 1 + \frac{\tau_{qj}}{\Delta t} \right)} (T_{j+1}^f - T_{j-1}^f) + \frac{\lambda_j \tau_{Tj}}{2h \Delta t \left( 1 + \frac{\tau_{qj}}{\Delta t} \right)} (T_{j+1}^{f-1} - T_{j-1}^{f-1}) \quad (4.3)$$

where the index  $j$  corresponds to 'heat flux nodes' (Fig. 3) belonging to the  $\Omega_m$  sub-domain.

The last equation allows one to construct similar formulas for the nodes  $i-1$ ,  $i+1$ , and then one obtains ( $\tau_{qi} = \tau_{qi-1} = \tau_{qi+1}$ ,  $\tau_{Ti} = \tau_{Ti-1} = \tau_{Ti+1}$ ,  $\lambda_i = \lambda_{i-1} = \lambda_{i+1}$ , of course)

$$q_{i-1}^f - q_{i+1}^f = \frac{\tau_{qi}}{\Delta t \left( 1 + \frac{\tau_{qi}}{\Delta t} \right)} (q_{i-1}^{f-1} - q_{i+1}^{f-1}) + \frac{\lambda_i \left( 1 + \frac{\tau_{Ti}}{\Delta t} \right)}{2h \left( 1 + \frac{\tau_{qi}}{\Delta t} \right)} (T_{i-2}^f - 2T_i^f + T_{i+2}^f) + \frac{\lambda_i \tau_{Ti}}{2h \Delta t \left( 1 + \frac{\tau_{qi}}{\Delta t} \right)} (T_{i-2}^{f-1} - 2T_i^{f-1} + T_{i+2}^{f-1}) \quad (4.4)$$

Putting (4.4) into (4.1), one has

$$\begin{aligned}
 c_i \frac{T_i^f - T_i^{f-1}}{\Delta t} &= \frac{\tau_{qi}}{2h\Delta t \left(1 + \frac{\tau_{qi}}{\Delta t}\right)} (q_{i-1}^{f-1} - q_{i+1}^{f-1}) + \\
 &+ \frac{\lambda_i \left(1 + \frac{\tau_{Ti}}{\Delta t}\right)}{4h^2 \left(1 + \frac{\tau_{qi}}{\Delta t}\right)} (T_{i-2}^f - 2T_i^f + T_{i+2}^f) + \\
 &- \frac{\lambda_i \tau_{Ti}}{4h^2 \Delta t \left(1 + \frac{\tau_{qi}}{\Delta t}\right)} (T_{i-2}^{f-1} - 2T_i^{f-1} + T_{i+2}^{f-1}) + Q_i^f
 \end{aligned} \tag{4.5}$$

or

$$A_i T_{i-2}^f - (1 + 2A_i) T_i^f + A_i T_{i+2}^f = D_i^f \tag{4.6}$$

where

$$A_i = \frac{\lambda_i \Delta t \left(1 + \frac{\tau_{Ti}}{\Delta t}\right)}{4h^2 c_i \left(1 + \frac{\tau_{qi}}{\Delta t}\right)} \tag{4.7}$$

and

$$D_i^f = B_i T_{i-2}^{f-1} - (1 + 2B_i) T_i^{f-1} + B_i T_{i+2}^{f-1} + C_i (q_{i+1}^{f-1} - q_{i-1}^{f-1}) - \frac{\Delta t}{c_i} Q_i^f \tag{4.8}$$

while

$$B_i = \frac{\lambda_i \tau_{Ti}}{4h^2 c_i \left(1 + \frac{\tau_{qi}}{\Delta t}\right)} \quad C_i = \frac{\tau_{qi}}{2h c_i \left(1 + \frac{\tau_{qi}}{\Delta t}\right)} \tag{4.9}$$

Let us assume that the contact temperatures  $T_i^f = T_{cm}^f$  at the boundary points  $x_m, m = 1, 2, \dots, M - 1$  are known. Then the temperature field at the time  $t^f$  results from the following systems of equations:

— first layer

$$\begin{aligned}
 T_0^f - T_2^f &= \frac{\frac{\tau_{T1}}{\Delta t}}{1 + \frac{\tau_{T1}}{\Delta t}} (T_2^{f-1} - T_0^{f-1}) \\
 A_i T_{i-2}^f - (1 + 2A_i) T_i^f + A_i T_{i+2}^f &= D_i^f \quad i = 2, 4, \dots, N_1 - 2 \\
 T_{N_1}^f &= T_{c1}^f
 \end{aligned} \tag{4.10}$$

— internal layers

$$\begin{aligned}
 T_{N_{m-1}}^f &= T_{cm-1}^f \\
 A_i T_{i-2}^f - (1 + 2A_i) T_i^f + A_i T_{i+2}^f &= D_i^f \\
 i &= N_{m-1} + 2, N_{m-1} + 4, \dots, N_m - 2 \\
 T_{N_m}^f &= T_{cm}^f
 \end{aligned} \tag{4.11}$$

— last layer

$$\begin{aligned}
 T_{N_{M-1}}^f &= T_{cM-1}^f \\
 A_i T_{i-2}^f - (1 + 2A_i) T_i^f + A_i T_{i+2}^f &= D_i^f \\
 i &= N_{M-1} + 2, N_{M-1} + 4, \dots, N - 2 \\
 T_{N-2}^f - T_N^f &= \frac{\frac{\tau_{TM}}{\Delta t}}{1 + \frac{\tau_{TM}}{\Delta t}} (T_N^{f-1} - T_{N-2}^{f-1})
 \end{aligned} \tag{4.12}$$

Finally, the problem of computations of contact temperatures will be explained. The continuity condition  $q_m(x, t) = q_{m+1}(x, t) = q_{cm}(x, t)$ , formula (3.3), leads to the equation  $x \in \Gamma_m$

$$\begin{aligned}
 \tau_{qm} \frac{\partial q_m(x, t)}{\partial t} + \lambda_m \frac{\partial T_m(x, t)}{\partial x} + \lambda_m \tau_{Tm} \frac{\partial^2 T_m(x, t)}{\partial t \partial x} &= \\
 = \tau_{qm+1} \frac{\partial q_{m+1}(x, t)}{\partial t} + \lambda_{m+1} \frac{\partial T_{m+1}(x, t)}{\partial x} + \lambda_{m+1} \tau_{Tm+1} \frac{\partial^2 T_{m+1}(x, t)}{\partial t \partial x}
 \end{aligned} \tag{4.13}$$

This formula should be written down using the finite difference convention, and then

$$\begin{aligned}
 \alpha_m T_{cm}^f &= \lambda_m \left(1 + \frac{\tau_{Tm}}{\Delta t}\right) T_{N_m-2}^f + \lambda_{m+1} \left(1 + \frac{\tau_{Tm+1}}{\Delta t}\right) T_{N_m+2}^{f-1} + \\
 &+ \frac{\lambda_m \tau_{Tm}}{\Delta t} (T_{cm}^{f-1} - T_{N_m-2}^{f-1}) + \lambda_m \tau_{Tm} (T_{cm}^{f-1} - T_{N_m-2}^{f-1}) + \\
 &+ \lambda_{m+1} \tau_{Tm+1} (T_{cm}^{f-1} - T_{N_m+2}^{f-1}) + \frac{2h}{\Delta t} (\tau_{qm+1} - \tau_{qm}) (q_{cm}^f - q_{cm}^{f-1})
 \end{aligned} \tag{4.14}$$

where

$$\alpha_m = \lambda_m \left(1 + \frac{\tau_{Tm}}{\Delta t}\right) + \lambda_{m+1} \left(1 + \frac{\tau_{Tm+1}}{\Delta t}\right) \tag{4.15}$$

In the place of  $q_{cm}^f$  and  $q_{cm}^{f-1}$ , the arithmetic means of heat flux values at the points  $N_{m-1}$ ,  $N_{m+1}$  are introduced. The starting point of computations consists in assumption that  $T_{cm}^0 = T_{cm}^1 = T_0$  and  $q_{cm}^0 = 0$ . Next, the system of equations (4.10), (4.11), (4.12) is solved and the heat fluxes at the odd internal nodes are found by means of equation (4.3). Finally, the contact temperatures  $T_{cm}^f$  are calculated using formula (4.14) and the next loop of computations can be realised. The method proposed is very quick and effective owing to application of the Thomas algorithm and decomposition of the domain.



### 5. Results of computations

To test the accuracy and effectiveness of the method proposed, at first the following task has been solved. The layer of thickness  $L = 10^{-4}$  and thermophysical parameters  $\lambda = 1$ ,  $c = 1$ ,  $\tau_q = 1/\pi^2 + 100$ ,  $\tau_T = 1/\pi^2 + 10^{-6}$ ,  $Q(x, t) = 0$  has been considered. For the data assumed, the problem described by equations (2.4), (2.5) and boundary-initial conditions in the form

$$\begin{aligned}
 T(0, t) = 0 & & T(L, t) = 0 \\
 T(x, 0) = \sin(10^4 \pi x) & & \left. \frac{\partial T(x, t)}{\partial t} \right|_{t=0} = -\pi^2 \sin(10^4 \pi x)
 \end{aligned}
 \tag{5.1}$$

has the following analytical solution (Dai and Nassar, 2001)

$$T(x, t) = \exp(-\pi^2 t) \sin(10^4 \pi x)
 \tag{5.2}$$

So, the domain considered has been divided in an artificial way into 4 parts of the same thickness, and ideal thermal contact between the sub-domains has been assumed. Using the algorithm presented in the previous sections on the assumption that  $h = 5 \cdot 10^{-7}$  and  $\Delta t = 0.0001$ , the transient temperature field has been found and the results have been compared with the exact solution. Both solutions are very close as shown in Fig. 4.

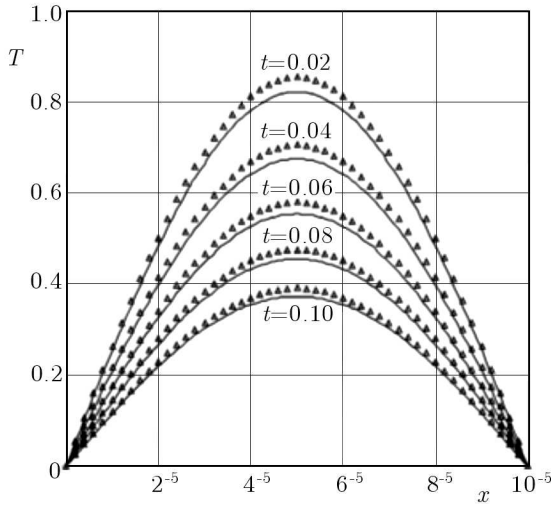


Fig. 4. Analytical (lines) and numerical (symbols) solutions

The second task is connected with the numerical solution presented in Dai and Nassar (2000) which concerns a two-layer domain (gold layer and chro-

mium layer of thicknesses 50 nm). In order to test the algorithm discussed, the domain considered has been divided into 4 parts ( $\Omega_1$  and  $\Omega_2$  correspond to the gold sub-domain,  $\Omega_3$  and  $\Omega_4$  correspond to the chromium sub-domain). The layers are subjected to short-pulse laser irradiation ( $R = 0.93$ ,  $I_0 = 13.7 \text{ J/m}^2$ ,  $t_p = 100 \text{ fs}$ ,  $\delta = 15.3 \text{ nm}$ ). Thermophysical parameters of the sub-domains are the following:  $\lambda = 317 \text{ W/(mK)}$ ,  $c = 2.4897 \text{ MJ/(m}^3\text{K)}$ ,  $\tau_q = 8.5 \text{ ps}$  ( $1 \text{ ps} = 10^{-12} \text{ s}$ ),  $\tau_T = 90 \text{ ps}$  (gold),  $\lambda = 93 \text{ W/(mK)}$ ,  $c = 3.2148 \text{ MJ/(m}^3\text{K)}$ ,  $\tau_q = 0.136 \text{ ps}$ ,  $\tau_T = 7.86 \text{ ps}$  (chromium). The mesh step:  $h = 1 \text{ nm}$ , time step:  $\Delta t = 0.005 \text{ ps}$ .

In Fig. 5, the temperature profiles (temperature rise above  $T_0 = 27^\circ\text{C}$ ) for the instants 0.2 ps and 0.25 ps are shown. The results of both solutions are close. The temperatures obtained using the algorithm presented here are bigger, indeed. It results from the fact that the laser interaction was probably approximated in a little different way, additionally the approach to the continuity conditions and the concept of decomposition were different, too.

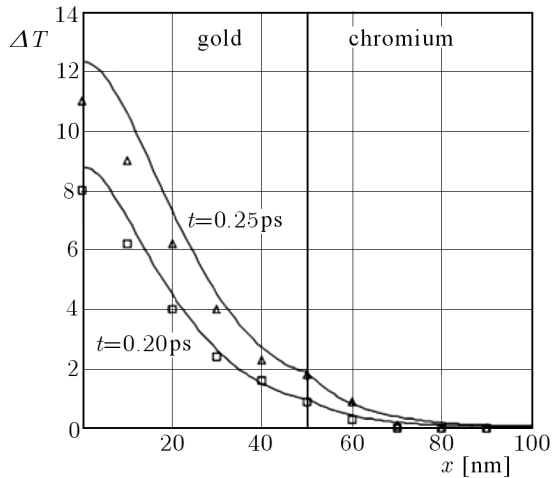


Fig. 5. Temperature profiles – comparison with solution (symbols) presented in Dai and Nassar (2000)

The last example concerns the alternating gold-chromium-gold-chromium layers. Thermophysical parameters of the materials are the same as previously, the laser characteristic is also the same.

In Fig. 6 the temperature profiles (temperature rise above  $T_0 = 27^\circ\text{C}$ ) for 1 – 0.4 ps, 2 – 0.6 ps, 3 – 0.8 ps and 4 – 1 ps are shown. Figure 7 illustrates the course of temperature at the surface subjected to laser heating ( $x = 0$ ) and the internal surfaces  $x = L_1$ ,  $x = L_1 + L_2$ .

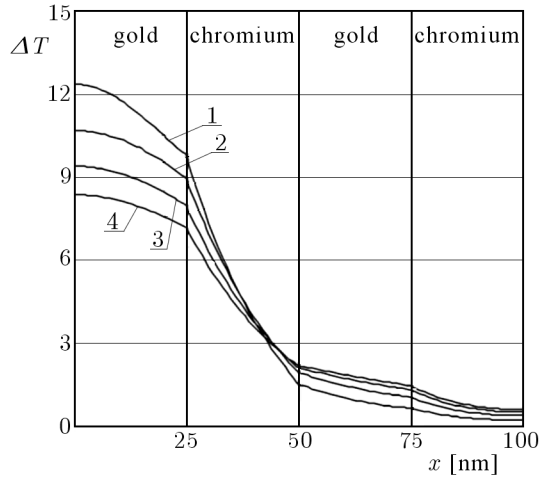


Fig. 6. Temperature profiles in the multi-layer domain

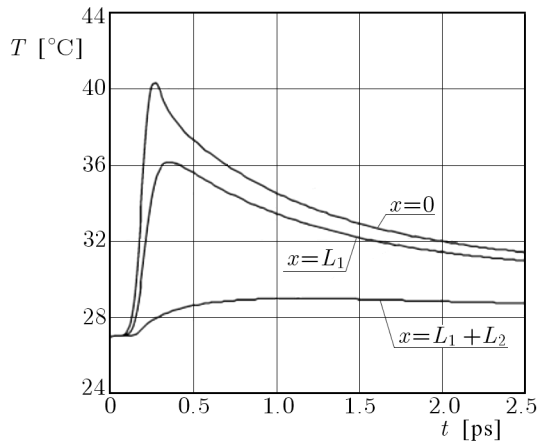


Fig. 7. Heating (cooling) curves at points selected from the domain  $\Omega$

### 6. Final remarks

The presented model based on the dual-phase-lag approach contains both the relaxation time  $\tau_q$  and additionally the thermalization time  $\tau_T$ . In literature concerning the microscale heat transfer, one can also find models for which only the relaxation time is taken into account. In this place the well known Cataneo equation can be mentioned. According to present opinions resulting mainly from experiments (Özişik and Tzou, 1994; Tank and Araki, 1999), it

seems that the assumption concerning a non-zero value of  $\tau_T$  gives results closer to real physical conditions of the microscale heat transfer.

The algorithm presented can be simply generalised for 2D or 3D tasks. The components determining  $q_2(x, t)$  and  $q_3(x, t)$  result then directly from the classical Fourier law. A numerical solution obtained in this way gives a possibility to analyse the influence of laser pulse distribution in the directions  $x_2$  and  $x_3$  on the course of heating and cooling processes in the domain considered.

The model presented here can be used for analysis of a heat transfer proceeding in multi-layered domains being a composition of an optional number of thin films with different parameters. The choice of materials considered in this paper results, first of all, from the available in literature input data. It seems that more close to real thermal conditions is the 2D model corresponding to an axially symmetrical domain, and this problem will be a subject of the future research.

#### *Acknowledgement*

The paper is a part of project MTKD-CT-2006-042468.

### References

1. AL-NIMR M.A., 1997, Heat transfer mechanisms during short duration laser heating of thin metal films, *International Journal of Thermophysics*, **18**, 5, 1257-1268
2. CHEN G., BORCA-TASCIUC D., YANG R.G., 2004, Nanoscale heat transfer, In: *Encyclopedia of Nanoscience and Nanotechnology*, Edited by H.S. Nalwa, Vol. X
3. CHEN J.K., BERAUN J.E., 2001, Numerical study of ultrashort laser pulse interactions with metal films, *Numerical Heat Transfer, Part A*, **40**, 1-20
4. DAI W., NASSAR R., 2000, A domain decomposition method for solving three-dimensional heat transport equations in a double-layered thin film with microscale thickness, *Numerical Heat Transfer, Part A*, **38**, 243-255
5. DAI W., NASSAR R., 2001a, A compact finite difference scheme for solving a one-dimensional heat transport equation at the microscale, *Journal of Computational and Applied Mathematics*, **132**, 431-441
6. DAI W., NASSAR R., 2001b, A finite difference scheme for solving a three-dimensional heat transport equation in a thin film with microscale thickness, *International Journal for Numerical Methods in Engineering*, **50**, 1665-1680

7. ESCOBAR R.A., GHAN S.S., JHON M.S., AMON C.H., 2006, Multi-length and time scale thermal transport using the lattice Boltzmann method with application to electronic cooling, *International Journal of Heat and Mass Transfer*, **49**, 97-107
8. KABA I.K., DAI W., 2005, A stable three-level finite difference scheme for solving the parabolic two-step model in a 3D micro-sphere heated by ultrashort-pulsed lasers, *Journal of Computational and Applied Mathematics*, **181**, 125-147
9. MAJCHRZAK E., MOCHNACKI B., 2004, *Numerical Methods. Theoretical Bases, Practical Aspects and Algorithms*, Publication of the Silesian University of Technology, Gliwice [in Polish]
10. MOCHNACKI B., SUCHY J.S., 1995, *Numerical Methods in Computations of Foundry Processes*, Polish Foundrymen's Technical Association, Cracow
11. ÖZİŞİK M.N., TZOU D.Y., 1994, On the wave theory in heat conduction, *Journal of Heat Transfer*, **116**, 526-535
12. SMITH A.N., NORRIS P.M., 2003, Microscale heat transfer, Chapter 18 in: *Heat Transfer Handbook*, John Wiley and Sons
13. TAMMA K.K., ZHOU X., 1998, Macroscale and microscale thermal transport and thermo-mechanical interactions: some noteworthy perspectives, *Journal of Thermal Stresses*, **21**, 405-449
14. TANG D.W., ARAKI N., 1999, Wavy, wavelike, diffusive thermal responses of finite rigid slabs to high-speed heating of laser-pulses, *International Journal of Heat and Mass Transfer*, **42**, 855-860
15. TZOU D.Y., 1995, A unified field approach for heat conduction from micro- to macro-scales, *Journal of Heat Transfer*, **117**, 8-16
16. TZOU D.Y., CHIU K.S., 2001, Temperature-dependent thermal lagging in ultrafast laser heating, *International Journal of Heat and Mass Transfer*, **44**, 1725-1734

**Symulacja numeryczna procesów cieplnych zachodzących  
w wielowarstwowych mikroobszarach poddanych działaniu ultrakrótkiego  
impulsu laserowego**

Streszczenie

W pracy przedstawiono model matematyczny, algorytm numeryczny i przykłady symulacji dotyczących przebiegu procesów cieplnych w wielowarstwowym mikroobszarze nagrzewanym ultraszybkim impulsem generowanym przez laser. Równanie opisujące przebieg procesu odpowiada modelowi z dwoma opóźnieniami wynikają-

cymi z czasu relaksacji i czasu termalizacji. Na etapie obliczeń numerycznych wykorzystano metodę różnic skończonych. Algorytm bazuje na sztucznej dekompozycji obszaru wielowarstwowego, przy czym wzajemne oddziaływania między warstwami uwzględniono poprzez założenie ciągłości strumienia ciepła i pola temperatury na powierzchniach kontaktu. Biorąc pod uwagę geometrię obszaru, rozpatrywano zadanie jednowymiarowe.

*Manuscript received September 22, 2008; accepted for print November 7, 2008*